Comparative Study of Piezoresistance Effect of Semiconducting Carbon Nanotube-Polydimethylsiloxane Nanocomposite Strain Sensor

Meehyun Lim[a], Jieun Lee[a], Dae Hwan Kim, Dong Myong Kim, Sungho Kim[*], and Sung-Jin Choi[*]

Abstract — **We comparatively study the performance of flexible strain sensors based on carbon nanotube (CNT)-Polydimethylsiloxane (PDMS) nanocomposites with different concentrations of CNTs. The semiconducting CNTs with high intrinsic gauge factor were employed for the sensor fabrications. A percolation network with a lower CNT concentration shows higher resistance changes in response to applied strains compared to those network with a higher CNT concentration. However, from a stability point of view, a lower concentration percolation network shows much worse characteristics than does a higher concentration percolation network. For the analysis of our observations, a 2-D percolation-based numerical model based on the Monte Carlo method was employed to understand the electrical and coupled electromechanical behaviors of CNT-PDMS nanocomposite strain sensors.**

I. INTRODUCTION

Strain sensors transduce mechanical deformations to electrical signals such as a change in the capacitance or resistance. Although commercially available strain sensors based on metal foils and semiconductors have matured as technologies with low fabrication costs, they generally possess very poor stretchability due to the brittleness of the sensing materials [1-3]. As an alternative to conventional strain sensors, a resistive type of strain sensors with high flexibility has been developed using nanomaterials and micro- and nano-structures. In particular, numerous reports based on percolation networks of nanomaterial/polymer composites, such as the composites of carbon nanotubes (CNTs) and Polydimethylsiloxane (PDMS), have been reported because the networks can maintain their electromechanical stability under condition of high strain [4, 5]. Despite these significant advances in strain sensors, the existing research based on the fundamental parameters influencing the piezoresistance effect in CNT-PDMS nanocomposites is still insufficient; thus, additional work is necessary. Notably, the concentration or density of CNTs in the nanocomposite can significantly affect the sensitivity and stability in the performance of strain sensors, but related studies have not been reported sufficiently.

M. Lim is with the Mechatronics R&D Center, Samsung electronics, Korea.

J. Lee, D. H. Kim, D. M. Kim, and S.-J. Choi are with School of Electrical Engineering, Kookmin University, Korea.

S. Kim is with the Department of Electrical Engineering, Sejong University, Korea

Corresponding author phone: +82-2-910-5543; fax: +82-2-910-4449; e-mail: sungho85kim@sejong.ac.kr and sjchoiee@kookmin.ac.kr

M. Lim[a] and J. Lee[a] equally contributed to this work.

In this paper, we experimentally investigate flexible strain sensors based on CNT-PDMS nanocomposites to study the important parameters that affect the sensitivity and stability of strain sensors. We utilized highly purified, pre-separated single-walled semiconducting CNTs as fillers in the strain sensors and selected the PDMS as our flexible substrate. For a comparative study of the piezoresistance effects of CNT-PDMS nanocomposite strain sensors, the concentration (or density) of CNTs was controlled by varying the number of spraying of CNTs onto the PDMS substrate. The resultant changes in piezoresistive resistance were thoroughly discussed and evaluated. Moreover, a 2-D percolation-based computational model based on the Monte Carlo method was developed to investigate the effect of CNT parameters on piezoresistive responses.

II. MODELING AND SIMULATION

To investigate the electrical and electromechanical properties of CNT-based nanocomposites, a 2-D percolation-based model was derived by randomly distributing straight 1-D CNTs of a Gaussian distributed predefined length (L_{CNT}). The concentrations of CNTs (N) and the dimensions of the 2-D thin film model (i.e., length, L, and width, W) were specified. We employed a 2-D model to reduce the computational demand. The location of CNTs was chosen by two-end points, (x_1, y_1) and (x_2, y_2), as represented in a Cartesian coordinate system. The first end point was determined by using a random number generator function in MATLAB, *rand*, and the other end point was then calculated using the L_{CNT} and a randomly generated CNT orientation (θ), as shown in Fig. 1 and given by Eqs. 1 and 2:

$$x_2 = x_1 + L_{CNT} \cdot \cos \theta \qquad (1)$$

$$y_2 = y_1 + L_{CNT} \cdot \sin \theta \qquad (2)$$

Upon generating the CNT networks in the model, the locations of CNT junctions were identified. The junction was defined as the location where CNTs intersected one another.
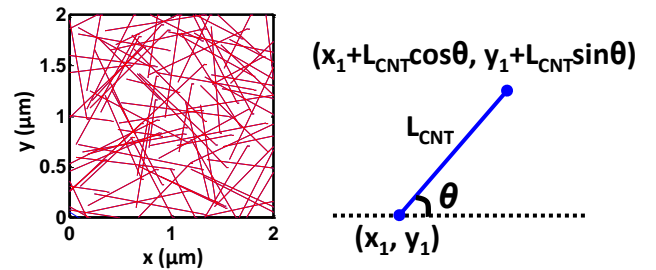

Fig. 1. Randomly generated CNT network in the representative 2-D unit area (2×2 μm^2) with a Gaussian distributed predefined CNT length (mean of L_{CNT} = 1 μm) and concentration (N = 100).
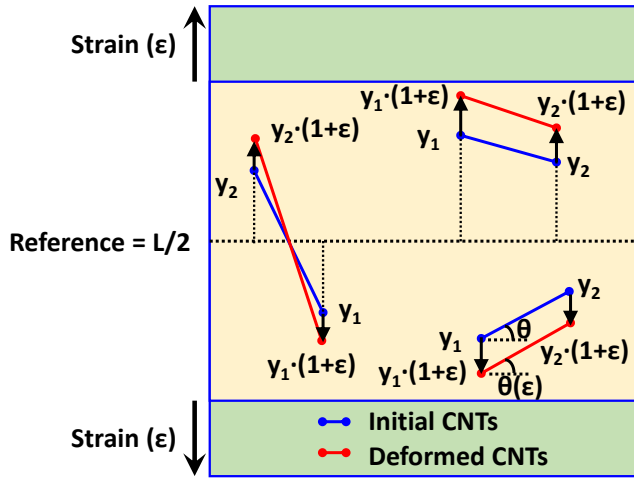
Fig. 2. Schematic illustration of updated coordinates and orientation under strain in the simulation.

Fig. 3. Randomly generated percolation network with the concentrations of CNTs (*N*) for different induced strains: (a) *N* = 60 and (b) *N* = 200. The red sticks represent the involvement of CNTs in the percolation network, and the blue sticks represent the non-involvement of CNTs in the percolation network.

Because tunneling between neighboring CNTs were not considered in this work, a junction corresponded to a direct CNT-to-CNT intersection (i.e., direct electrical contact). In addition, because the CNTs employed in this work were assumed to be straight, they can also be expressed as linear equations. Therefore, the locations of junctions were found by simply solving sets of linear equations, and the results were stored in a junction matrix. Then, upon assuming the resistance of the CNTs per unit length (R_{CNT}), the resistance that is connected by CNTs between junctions was calculated. The final step was to calculate the resistance of the entire CNT network film. For this purpose, a combination of Kirchhoff's current law and Ohm's law were utilized for Nodal analysis.

The CNT-PDMS nanocomposite strain sensor subjected to mechanical deformation results in changes in electrical resistance. For this simulation, the CNT percolation model formulated previously was subjected to uniaxial tensile strain to quantify the electromechanical properties. For this specific implementation, the tensile strain was applied in the direction of the *y*-axis. The coordinate at *y* = 0.5*L* was fixed, and the remainder of the film deformed accordingly and relative to this point, as shown in Fig. 2. The fundamental assumption for updating coordinates was that the CNTs experienced perfect mechanical coupling with the polymer matrix. Therefore, the applied strain (ε) deformed both the CNTs and PDMS matrix in the same way, and no stress concentrations or discontinuities existed. The applied strain deformed each CNT and altered the orientation, and the coordinate was then updated accordingly using Eqs. 3 and 4.

$$y = y_0 \cdot (1 + \varepsilon) \tag{3}$$

$$\theta = \tan^{-1}[(1 + \varepsilon) \cdot \tan \theta_0] \tag{4}$$

where y_0 and θ_0 are the initial *y*-coordinate and CNT orientation, respectively. We assume that the initial *x*-coordinate was not changed under strain.

Fig. 3 shows a deformed CNT percolated network with updated coordinates in a 2-D initial square cell for applied tensile strains of 0% (initial unstrained case), 25%, 50%, 75%, and 100%. For higher concentrations of CNTs (*N* = 200), all of CNTs were involved in the electrical percolation connected through top and bottom electrodes, even with a higher strain of
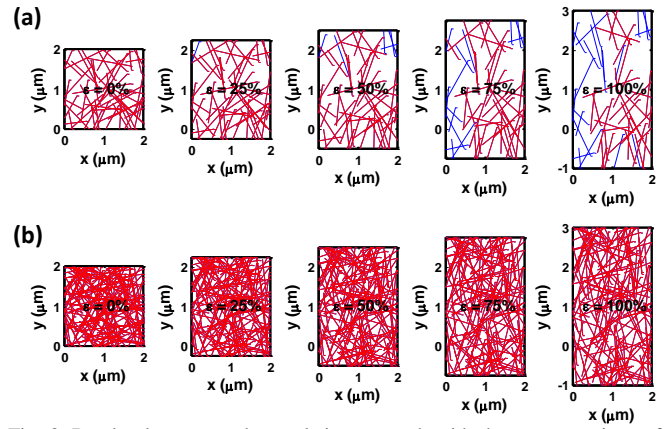
100%. Thus, it is predicted that the resistance of the entire film was not significantly changed. In this case, the film's responses only depend on changes in the CNT length. However, for lower concentration of CNTs (*N* = 60), the CNTs involved in the percolation were clearly reduced with higher strain such that the responses of the entire film were expected to be remarkably observed.

The resistance of the entire CNT network was then recalculated after inducing strain, following the same procedure mentioned previously. It should be noted that only models with CNT concentrations that exceeded the percolation threshold were considered. The model's resistance was then correlated to different magnitudes of applied tensile strains to study the electromechanical properties. The model aimed to simulate a representative element of an actual thin film rather than the entire film subjected to electromechanical testing.

From a large number of simulations based on various models in a 2-D square cell, we investigated the electromechanical properties of the CNT percolated network thin film by calculating how the electrical properties varied with different magnitudes of applied strain. Fig. 4 shows the percentage of CNTs involved in the percolation network versus the concentration of CNTs for different strains. Each point was simulated by 50 runs. From the results, it is globally observed that as the CNT concentration increases, most of the CNTs take part in the percolation network path (approaching to 100%), regardless of induced strain. For the lower CNT concentration (*N* = 60), 98.1% of the CNTs were initially involved in the percolation path (for the unstrained case), but for 75% induced strain, the percentage of CNTs involved in the percolation path was reduced to 62.1%. However, for the higher CNT concentration (*N* = 200), only 0.2% CNTs, i.e., four CNTs, were removed from the percolation network, so a minimal response in resistance to the strain can be expected.

Upon executing all of the different numerical simulations that employed different concentrations of CNTs for various induced strains, the results are summarized in Fig. 5. Each data was also determined from 50 simulation runs. Fig. 5a shows the normalized change in resistance of the film, defined as $\Delta R_{mean}/R_{0,mean}$ where $R_{0,mean}$ is the mean of initial unstrained resistance for simulations and ΔR_{mean} is the mean of the change
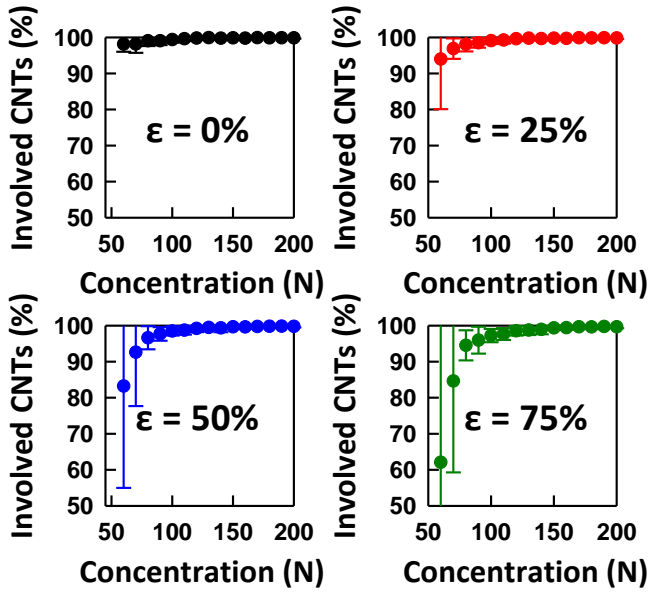
Fig. 4. Percentage of CNTs involved in the percolation network versus concentrations of CNTs. The induced strains are 0% (for the unstrained case), 25%, 50%, and 75%. Each point was simulation by 50 runs.
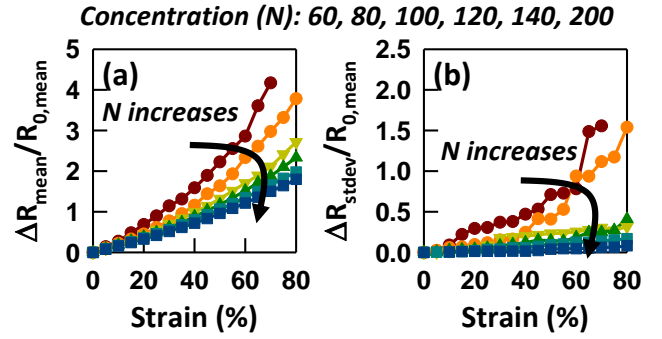

Fig. 5. (a) Strain sensitivity and (b) normalized standard error versus induced strain for different CNT concentrations. Each point was simulated by 50 runs.

in resistance for simulations between the strained and unstrained cases, versus induced strain. The trend in which the normalized resistance change increases with the strain is clearly observed for all concentrations of CNTs. Importantly, the strain sensitivity, i.e., $\Delta R_{mean}/R_{0,mean}$, decreased as the CNT concentration increased. Moreover, the normalized change in resistance was saturated with the CNT concentration. As previously mentioned, for the low CNT concentration, upon stretching, large portion of CNTs was separated apart within the percolation network, i.e., the number of CNTs involved in the percolation network were greatly reduced, resulting in largely increased film resistance. Therefore, the sensitivity is much higher in the low concentration network because fewer parallel conduction pathways contribute to the electrical conductivity under higher strain.

The simulation results also show that the linearity as well as the strain sensitivity can be tuned by adjusting the CNT concentration to needs of individual applications. The low CNT concentration with nonlinear responses are appropriate for high sensitivity with low strain applications. On the other hand, for very high strain applications with acceptable sensitivity, high CNT concentration can be utilized due to high linearity. Note that the nonlinearity in low CNT concentration resulted from the change of topology of percolating CNTs, as previously shown in Fig. 3. The CNT percolation network with low concentration transforms from homogeneous network to inhomogeneous network with emerging bottleneck locations that critically limit the electrical current path. In contrast, highly linear response was observed in the high CNT concentration due to dense CNT percolation network. In this case, there was no bottleneck locations for electrical current even for high strain up to 80% due to high number of CNTs.

Moreover, at the point of stability in the strain sensor, it is expected that the lower CNT concentration exhibits worse characteristics than the higher CNT concentration. Fig. 5b shows the normalized standard error for 50 simulation runs

versus the applied strains for different CNT concentrations. For the low CNT concentration, the standard error during the simulations is quite large compared to that of the high CNT concentration, indicating poor stability during the induced strain. That is, fewer connections of CNTs in the lower concentration network were not maintained well under high strain, which degraded the stability of the sensor with a lower CNT concentration.

III. EXPERIMENT

Based on the simulation results, we fabricate a CNT-PDMS nanocomposite strain sensor to investigate the piezoresistance effect for different CNT concentrations in the percolation network. Our strain sensor has the stacked sandwich-like structure of CNTs and PDMS layers. This three-layer stacked strain sensor showed improved stability in terms of sensor response. First, a thin and stretchable PDMS substrate with a thickness of 0.5 mm was treated by UV O_3 to make the surface hydrophilic. Then, the surface was functionalized with a 0.1 g/ml poly-L-lysine solution to form an amine-terminated layer, which acted as an effective adhesion layer for the deposition of CNTs. The substrate was then rinsed with deionized (DI) water. Subsequently, the CNT network channel was formed using airbrush spraying of 0.01 mg/ml 90% semiconducting-enriched CNT solution for several times, followed by thoroughly rinsing with isopropanol and DI water. Then, two terminals were formed by placing Ag paste on the end points of the CNT percolation network, followed by attaching Cu tape at each terminal. Finally, top layer of the PDMS was attached and pasted using the PDMS solution, followed by curing at 80 ℃ for 3 hours. The process is shown schematically in Fig. 6.
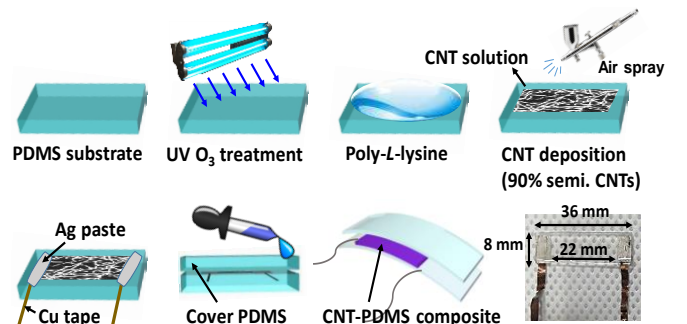

Fig. 6. Schematic of the process of CNT-PDMS nanocomposite strain sensor fabrication. The final structure of the sensor is also shown.
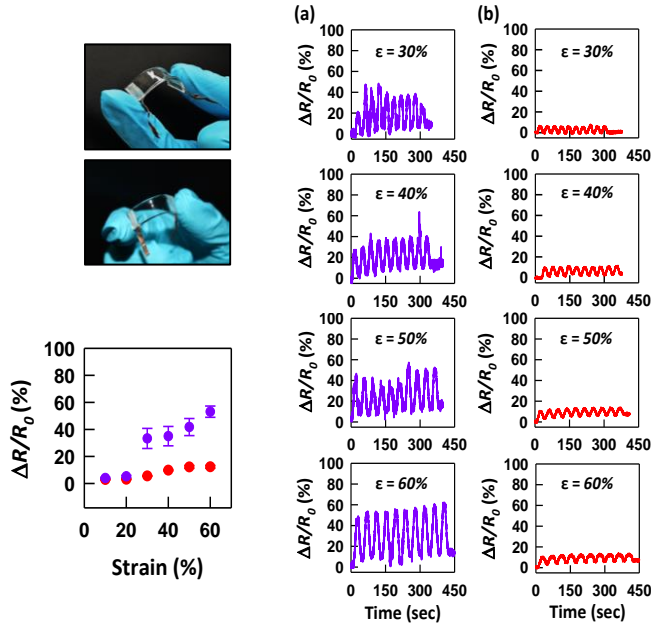
Fig. 7. Time-dependent normalized resistance changes ($\Delta R/R_0$), i.e., strain sensitivity, of the three-layer stacked CNT-PDMS nanocomposite strain sensor with different CNT concentrations: (a) lower CNT concentration case (Initial resistance = 3.06 MΩ at 1 V) and (b) higher CNT concentration case (Initial resistance = 136 kΩ at 1 V).

We evaluated the effects of different CNT concentrations in the CNT percolation network on sensor performance. Fig. 7 shows the measured time-dependent normalized change in resistance ($\Delta R/R_0$) of the three-layer stacked CNT-PDMS nanocomposite sensor. We used two deposition conditions for the formation of the CNT percolation network. The initial resistances at induced voltage of 1 V are 3.06 MΩ and 136 kΩ for the two sensors, respectively. Each sensor was subjected to strain (ε) ranging from 0% to 60% (ε is a percentage of strain defined as $\Delta L/L_0$ where L_0 is an initial length of sensing layer, 9 mm, and ΔL is a changed length by applied tensile strain, 0−5.4 mm), with 10 stretching/releasing cycles. It should be noted that the CNT concentration significantly affected the electrical responses. The sensor with a higher initial resistance (3.06 MΩ), i.e., lower CNT concentration, had a higher sensitivity, but poorer stability. The relatively high sensitivity observed in our strain sensor can be attributed to high gauge factor of intrinsic semiconducting CNTs in percolation network [6]. On the other hand, the sensor with a lower initial resistance (136 kΩ), i.e., higher CNT concentration, had a lower sensitivity, but better stability. The increase in stability and decrease in sensitivity with increasing CNT concentration is due to changes in the level of electrical transport depending on the average distance between CNTs, as expected in the simulation. Increasing the CNT concentration resulted in an increased number of junctions between CNTs, which enhanced the current flow. Therefore, increased junctions increased the conductance and, in turn, relative resistance; that is, the sensitivity decreased with higher CNT concentration. However, more junctions between CNTs were well maintained under straining during stretching, which enhanced the stability of the sensor with a higher CNT concentration. Therefore, it is concluded that the sensitivity and stability of the strain sensors can be tuned simply by adjusting the concentration of CNTs and deposition parameters.

IV. CONCLUSION

We demonstrate the performance of a semiconducting CNT-PDMS nanocomposite strain sensor with a sandwich-like structure. It was observed that the lower concentration of CNTs resulted in higher sensitivity, but poorer stability. In contrast, a higher CNT concentration showed lower sensitivity, but improved stability. This observation was investigated through using the implementation of a 2-D percolation-based numerical model based on Monte Carlo method.

REFERENCES

[1] M. Amjadi, A. Pichitpajongkit, S. Lee, S. Ryu and I. Park, "Highly stretchable and sensitive strain sensor based on silver nanowire-elastomer nanocomposite," *ACS Nano*, vol. 8, no. 5, pp. 5154–5163, Apr. 2014.

[2] C. Yan, J. Wang, W. Kang, M. Cui, X. Wang, C. Y. Foo, K. J. Chee, P. S. Lee, "Highly Stretchable Piezoresistive Graphene–Nanocellulose Nanopaper for Strain Sensors," *Adv. Mater.*, vol. 26, no. 13, pp. 2020–2027, Apr. 2014.

[3] M. Hempel, D. Nezich, J. Kong, M. Hofmann, "A Novel Class of Strain Gauges Based on Layered Percolative Films of 2D Materials," *Nano Lett.*, vol. 12, no. 11, pp. 5714–5718, Oct. 2012.

[4] T. Yamada, Y. Hayamizu, Y. Yamamoto, Y. Yomogida, A. Izadi-Najafabadi, D. N. Futaba, and K. Hata, "A stretchable carbon nanotube strain sensor for human-motion detection," *Nat. Nanotechnol.*, vol. 6, pp. 296–301, Mar. 2011.

[5] L. Cai, L. Song, P. Luan, Q. Zhang, N. Zhang, Q. Gao, D. Zhao, X. Zhang, M. Tu, F. Yang, W. Zhou, Q. Fan, J. Luo, W. Zhou, P. M. Ajayan, and S. Xie, "Super-stretchable, Transparent Carbon Nanotube-Based Capacitive Strain Sensors for Human Motion Detection," *Sci. Rep.*, vol. 3, pp. 1–3, Oct. 2013.

[6] J. Cao, Q. Wang, and H. Dai, "Electromechanical Properties of Metallic, Quasimetallic, and Semiconducting Carbon Nanotubes under Stretching," *Phys. Rev. Lett.*, vol. 90, no. 15, pp. 157601–1–4, Apr. 2003.